AGU PUBLICATIONS

JGR

Journal of Geophysical Research: Oceans

RESEARCH ARTICLE

10.1002/2013JC009525

Key Points:
- Pacific and Indian Oceans are connected through ITF and Tasman leakage
- Both pathways are important for global circulation but are not correlated
- A Lagrangian analysis of pathways finds effect of ENSO in Archipelago

Supporting Information:
- Supplementary video file

Correspondence to:
E. van Sebille,
e.vansebille@unsw.edu.au

Citation:
van Sebille, E., J. Sprintall, F. U. Schwarzkopf, A. S. Gupta, A. Santoso, M. H. England, A. Biastoch, and C. W. Böning (2014), Pacific-to-Indian Ocean connectivity: Tasman leakage, Indonesian Throughflow, and the role of ENSO, *J. Geophys. Res. Oceans*, *119*, 1365–1382, doi:10.1002/2013JC009525.

Received 21 OCT 2013
Accepted 4 FEB 2014
Accepted article online 11 FEB 2014
Published online 24 FEB 2014

Pacific-to-Indian Ocean connectivity: Tasman leakage, Indonesian Throughflow, and the role of ENSO

Erik van Sebille[1], Janet Sprintall[2], Franziska U. Schwarzkopf[3], Alex Sen Gupta[1], Agus Santoso[1], Matthew H. England[1], Arne Biastoch[3], and Claus W. Böning[3]

[1]ARC Centre of Excellence for Climate System Science & Climate Change Research Centre, University of New South Wales, Sydney, New South Wales, Australia, [2]Scripps Institution of Oceanography, La Jolla, California, USA, [3]GEOMAR Helmholtz-Zentrum für Ozeanforschung Kiel, Kiel, Germany

Abstract The upper ocean circulation of the Pacific and Indian Oceans is connected through both the Indonesian Throughflow north of Australia and the Tasman leakage around its south. The relative importance of these two pathways is examined using virtual Lagrangian particles in a high-resolution nested ocean model. The unprecedented combination of a long integration time within an eddy-permitting ocean model simulation allows the first assessment of the interannual variability of these pathways in a realistic setting. The mean Indonesian Throughflow, as diagnosed by the particles, is 14.3 Sv, considerably higher than the diagnosed average Tasman leakage of 4.2 Sv. The time series of Indonesian Throughflow agrees well with the Eulerian transport through the major Indonesian Passages, validating the Lagrangian approach using transport-tagged particles. While the Indonesian Throughflow is mainly associated with upper ocean pathways, the Tasman leakage is concentrated in the 400–900 m depth range at subtropical latitudes. Over the effective period considered (1968–1994), no apparent relationship is found between the Tasman leakage and Indonesian Throughflow. However, the Indonesian Throughflow transport correlates with ENSO. During strong La Niñas, more water of Southern Hemisphere origin flows through Makassar, Moluccas, Ombai, and Timor Straits, but less through Moluccas Strait. In general, each strait responds differently to ENSO, highlighting the complex nature of the ENSO-ITF interaction.

1. Introduction

Water in the upper ocean flows from the Pacific to the Indian Ocean as part of the upper limb of the global thermohaline circulation. There are two routes for this Pacific-to-Indian exchange: either around the north of Australia via the Indonesian Archipelago, or around the south of Australia. The first of these routes, the so-called Indonesian Throughflow, has been the subject of recent and ongoing monitoring efforts [*Sprintall et al.*, 2009; *Gordon et al.*, 2010]. The second route, the Tasman leakage [*Speich et al.*, 2002], is far less understood, although there have been some recent advances in the understanding of its dynamics [*van Sebille et al.*, 2012].

Numerical experiments, in which the Indonesian Throughflow is artificially blocked, have shown an increase in Tasman leakage [e.g., *Hirst and Godfrey*, 1993; *Wajsowicz and Schneider*, 2001; *Lee et al.*, 2002; *Song et al.*, 2007; *Santoso et al.*, 2011; *Le Bars et al.*, 2013]. This suggests that in the most extreme case, there is compensation between the Indonesian Throughflow and Tasman leakage. What is not known, however, is how and whether these two interocean transports compensate each other in more realistic configurations, and how their variabilities at interannual time scales might be related.

The Indonesian Throughflow has been studied for many years, culminating in the early 2000s in an extensive field campaign known as the International Nusantara Stratification and Transport (INSTANT) experiment [*Sprintall et al.*, 2004; *Gordon*, 2005]. The INSTANT campaign led to an increase in the understanding of the variability of Indonesian Throughflow and the dynamics that drive that variability. Both El Niño Southern Oscillation (ENSO) in the Pacific Ocean and Indian Ocean variability appear to play a role in setting the magnitude of the Indonesian Throughflow on interannual time scales [*Meyers*, 1996; *England and Huang*, 2005; *Potemra and Schneider*, 2007; *Du and Qu*, 2010; *Yuan et al.*, 2011]. Changes in the tropical Pacific trade winds on both interannual and longer term decadal time scales generate large-scale planetary waves that pass through the Indonesian Seas [*Wijffels and Meyers*, 2004; *McClean et al.*, 2005; *Cai et al.*, 2011; *Feng et al.*,

2011; *Schwarzkopf and Böning*, 2011]. As the Indonesian Throughflow transports large amounts of heat and freshwater into the Indian Ocean [*Vranes et al*., 2002; *Talley*, 2008], its existence plays a role in regulating the global climate [*Hirst and Godfrey*, 1993], even influencing the behavior of ENSO [*Koch-Larrouy et al*., 2009; *Santoso et al*., 2011, 2012].

The subpolar component of the interbasin exchange, the Tasman leakage (or Tasman outflow), moves water from the Pacific to the Indian Ocean via a route around the southern tip of Tasmania, south of Australia. It forms part of the supergyre [*Speich et al*., 2002; *Cai*, 2006] that encompasses all three subtropical basins in the Southern Hemisphere. Water from the western subtropical Pacific flows southward in the East Australian Current (EAC), the western boundary current of the South Pacific subtropical gyre, until that current reaches the Tasman Front at 35°S [see also *Ridgway and Dunn*, 2003; *van Sebille et al*., 2012]. At that point, most of the water within the EAC turns eastward and flows toward New Zealand forming the southern limb of the subtropical gyre. Occasionally, however, large eddies are shed at the Tasman Front, which then move southward along the Australian seaboard, carrying with them some of the subtropical waters [*Suthers et al*., 2011]. Part of the water within the eddies rounds Tasmania, after which point some of it flows westward across the Great Australian Bight and finally into the Indian Ocean [*Ridgway and Dunn*, 2007].

As the Tasman leakage rounds Tasmania, it can flow westward in only a narrow band. This is because the vigorous Antarctic Circumpolar Current flows in the opposite direction $<$200 km south of Tasmania, at the Subtropical Front. It appears that this narrow passage acts as a bottleneck, where the amount of Tasman leakage becomes smaller when the Subtropical Front shifts northward [e.g., *Rintoul and Sokolov*, 2001]. This bottleneck effect, together with the fact that EAC eddies play a crucial role in moving Tasman leakage southward along Australia's eastern seaboard, suggests that the winds in the Southern and Pacific Oceans might modulate the amount of Tasman leakage. This sensitivity to external drivers is also apparent in a high-resolution model pilot study that found large variability in Tasman leakage [*van Sebille et al*., 2012].

The mean volume transport of the Tasman leakage is much smaller than that of the Indonesian Throughflow, approximately 4 Sv [*van Sebille et al*., 2012] and 13 Sv [*Gordon et al*., 2010], respectively. Nevertheless, there are reasons why one might still expect a relationship between Indonesian Throughflow and Tasman leakage variability on interannual and longer time scales. One hypothesis is that the bifurcation of the South Equatorial Current in the Coral Sea determines the distribution between northward and southward flows, so that the two streams might compensate in their variability. This variability is particularly important, as models suggest that the recently detected long-term trends observed in the large-scale wind patterns in both the tropical and subtropical/subpolar Pacific drive distinctive changes in the Pacific circulation that subsequently impact the interocean exchange [*Cai et al*., 2011; *Feng et al*., 2011; *Schwarzkopf and Böning*, 2011; *van Sebille et al*., 2012]. Furthermore, it has been shown [e.g., *McCreary et al*., 2007] that a sudden opening of the Indonesian Throughflow affects the circulation all around Australia, including south of Tasmania and hence will likely have an impact on Tasman leakage. While this might be an extreme case, it does show that the two Pacific-to-Indian interocean exchanges are (at least weakly) coupled on long time scales. Finally, there seems to be an ENSO signal in the East Australian Current [*Holbrook et al*., 2011]. If these ENSO signals transfer into the Tasman leakage, then the timing of some of the variability of both the Indonesian Throughflow and Tasman leakage may be controlled by ENSO.

The interannual variations of the pathways, for example, how the Indonesian Throughflow is partitioned through the various passages according to the phases of ENSO, are not well understood. This is due to the highly complex bathymetry of the Indonesian Archipelago, making it difficult for any direct or indirect observing systems to fully sample the spatial and temporal characteristics of the flows. In addition, the distribution and associated variability of Indonesian Throughflow source waters of northern and southern Pacific origin at various depth levels have very different properties [*Godfrey et al*., 1993; *Gordon*, 1995; *Valsala et al*., 2011]. Resolving these properties is important in light of the influence of local SSTs on different rainfall regimes over the Indonesian region [*Aldrian and Susanto*, 2003; *England et al*., 2006] which can in turn affect ENSO evolution [*Annamalai et al*., 2010]. Given the lack of suitable sustained observations, such information can only be gleaned from high-resolution ocean models that resolve the narrow passages within the Indonesian Seas.

In this study, we investigate the pathways of both the Tasman leakage and the Indonesian Throughflow using an eddy-resolving ocean model. We compare time series of the two leakages and examine the origin

and fate of their respective water mass sources from the Pacific through to the Indian Ocean. We do this in a Lagrangian framework as this means that conditional pathways can be investigated (i.e., we can set conditions on the origin, fate, and route of particles). In particular, this allows us to identify interbasin Tasman leakage (i.e., where particles need to start in the Pacific Ocean and end in the Indian Ocean, travelling south of Australia, see also section 2.3). The goal is to examine the dynamics and interplay of the interocean exchange between the Pacific and Indian Oceans via both the tropical (Indonesian Throughflow) and subpolar (Tasman leakage) pathways, which both are important chokepoints in the global large-scale circulation.

2. Methods

2.1. The Ocean General Circulation Model

In this study, the Pacific-to-Indian Ocean exchanges are investigated in the high-resolution TROPAC01 model. This model configuration, developed in the European Drakkar cooperation [*Barnier et al*., 2007], based on the NEMO [v3.2 *Madec*, 2008] code, is a 1/10° horizontal resolution model of the tropical Indo-Pacific region (spanning the area from 73°E–63°W to 49°S–31°N), nested within a half-degree global ocean/sea-ice model. The nesting is done using the AGRIF tool, providing an immediate link between the global and nested grids [*Debreu et al*., 2008]. In the vertical, TROPAC01 has 46 z-levels: 10 levels in the top 100 m and a maximum layer thickness of 250 m at depth, whereby bottom cells are allowed to be partially filled [*Barnier et al*., 2006]. The bathymetry within the nested region is based on ETOPO2, where special care is taken to represent the Indonesian Passages as realistically as possible. The atmospheric forcing builds on the CORE reanalysis products developed by *Large and Yeager* [2009] covering the period 1948–2009 and is applied via bulk air-sea flux formulae.

For the analysis, 50 years (1960–2009) of data from the hind-cast experiment are used, with temporal means available every 5 days. *van Sebille et al*. [2009] have shown that 5 day temporal means are of sufficiently high resolution to study Lagrangian connectivity in high-resolution ocean models. As the focus is on the region around Australia only, and to be consistent with the Ocean General Circulation Model For the Earth Simulator (OFES) analysis of the Tasman leakage by *van Sebille et al*. [2012], only data in a subdomain between 90°E–170°W and 49°S–15°N are used. One important difference between the TROPAC01 model used here and the OFES model used by *van Sebille et al*. [2012], is that the TROPAC01 run is 20 years longer, which means there is more scope to study interannual to decadal variability.

The model reproduces many of the circulation features in the region, as can be seen when comparing the simulated sea-surface height with AVISO altimetry data for the overlapping time period of 1993–2009 (Figure 1). However, there are certain biases, such as the extended tongue of elevated sea surface height in the model Indian Ocean at around 15°S, which is confined to the far eastern basin in the altimetry data. There are also some differences in the Indonesian Archipelago, although these may be partly the result of poor satellite performance in that region. The variability of sea surface height (Figures 1b and 1d) in TROPAC01 is in particularly good agreement with the altimetry measurements, with slight underestimations in the more energetic regions such as the Tasman Sea eddy corridor [*Everett et al*., 2012] and the Arafura Sea.

2.2. The Lagrangian Particle Model

The interocean pathways themselves can most aptly be studied by tracking virtual Lagrangian particles in the model velocity fields [e.g., *van Sebille et al*., 2010]. Here we use the Connectivity Modelling System (CMS) v1.1 [*Paris et al*., 2013] to integrate the virtual particles in the three-dimensional and time-evolving flow. The particles are computed offline using the velocity data on the TROPAC01 native grid and using the velocity output on 5 day resolution. Two sets of particle experiments are undertaken: one to track the Indonesian Throughflow and one to track the Tasman leakage.

To examine the Indonesian Throughflow, particles are released between the surface and 1500 m depth along two lines in the Pacific Ocean: at 14°N between 108°E and 171°W, and at 171°W between 14°N and 35°S. Both of these sections are shown as green lines in Figure 2a. Note that, in this definition, we exclude water from south of 35°S at 171°W. As will be shown later (Figures 3 and 7), all water south of 25°S in the Pacific will either recirculate in that region or arrive in the Indian Ocean via the Tasman leakage. As such,

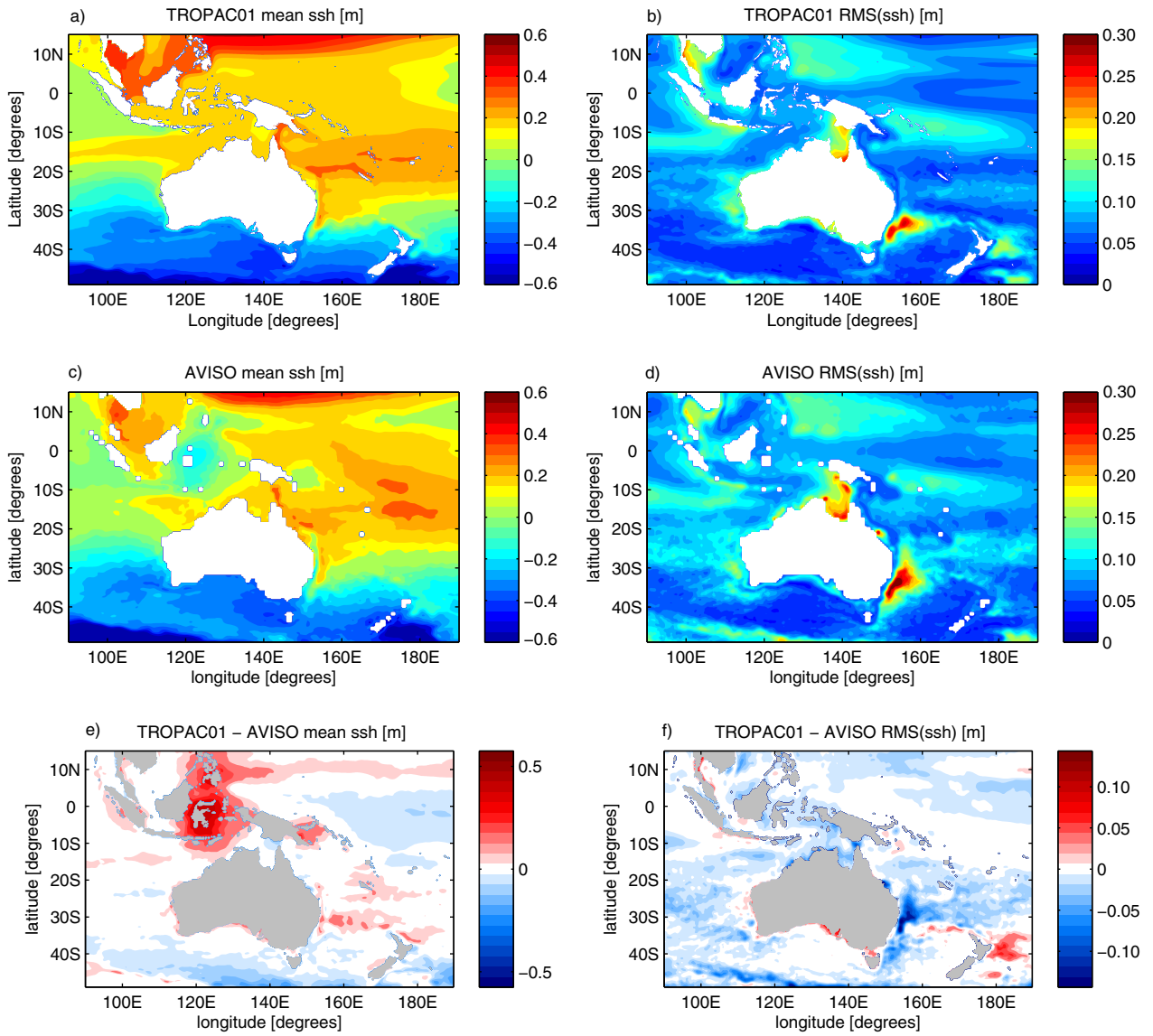

Figure 1. Evaluation of the TROPAC01 model, by comparing the model sea surface height data for the period 1993–2009 to AVISO altimetry data. The figure shows the extent of the domain as used in this study. The model (a) mean sea surface height and (b) its variability are compared to the (c) mean and (d) variability in the altimetry data. The difference between the model and altimeter sea surface height is shown in Figures 1e and 1f.

limiting the release of Indonesian Throughflow water to north of 35°S does not result in an underestimation of Indonesian Throughflow.

The particles are released every 5 days, at 100 m intervals in depth between 0 and 1500 m, and at every 0.5° in latitude. These time-space intervals of release were chosen to obtain unbiased estimates of transport values along the two transport pathways, while also being constrained by computational resources: sensitivity tests (not shown) demonstrate that the number of particles used here suffices to robustly study the Indonesian Throughflow pathways.

The particles are assigned a transport equal to the local velocity in the release grid cell (which is larger than the internal model grid cell) times the area of that grid cell [see also *van Sebille et al*., 2010, 2012]. The particles are then tracked forward in time until they reach one of the domain boundaries. Note that this means that particles released in earlier years can spend more time in the domain, something that needs to be taken into account when analyzing the results (see also section 3.3). Along their pathway, the particles maintain their original transport. This method of tagging particles with a transport at release has been

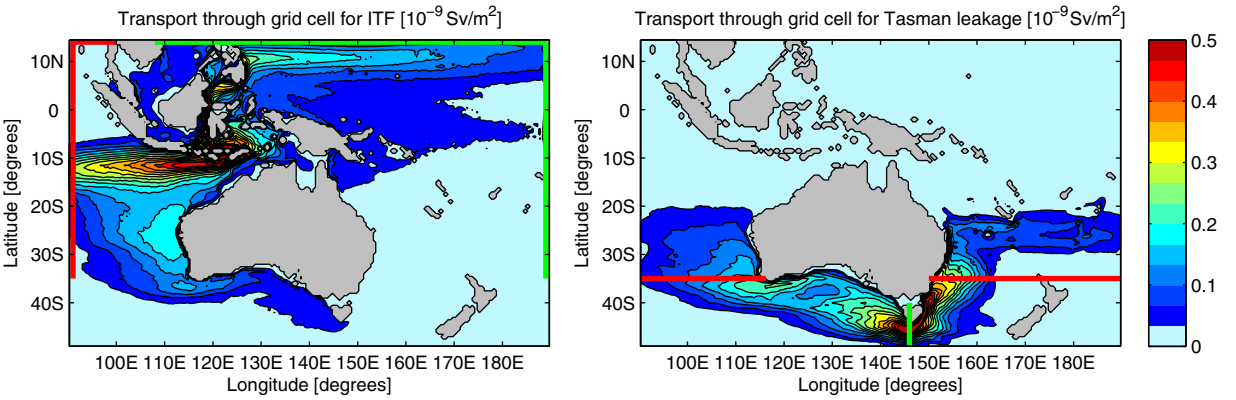

Figure 2. Maps of depth-integrated transport (in 10^{-9} Sv/m^2) carried by (a) the Indonesian Throughflow and (b) the Tasman leakage particles, on a 0.5 × 0.5 degree grid. Higher values mean that more particles enter those grid cells at any depth and at any point through the experiment. The green lines are the sections where particles are released. The red lines are sections that the particles reach in order to be considered either Indonesian Throughflow or Tasman leakage. In the latter case, the particles have to reach the section in the Indian Ocean when integrated forward in time and the section in the Pacific Ocean when integrated backward in time.

utilized extensively before [e.g., *Döös*, 1995; *Speich et al*., 2002, 2007; *van Sebille et al*., 2010], and in this study, we will show (Figures 5 and 7) that the method yields transports in very good agreement with the local Eulerian transport through the Indonesian Passages.

To examine the Tasman leakage, particles are released along a meridional section at 146°E, between the southern tip of Australia and the southern boundary of the domain at 49°S (the green line in Figure 2b). Note that there is no significant transport through Bass Strait between Tasmania and the mainland of Australia as it is <50 m deep. Because the core of Tasman leakage is rather narrow south of Tasmania, the particles are released closer together than in the case of the Indonesian Throughflow, with 0.2° spacing in latitude and only 50 m spacing in depth over the top 3000 m. The particles are then tracked both forward

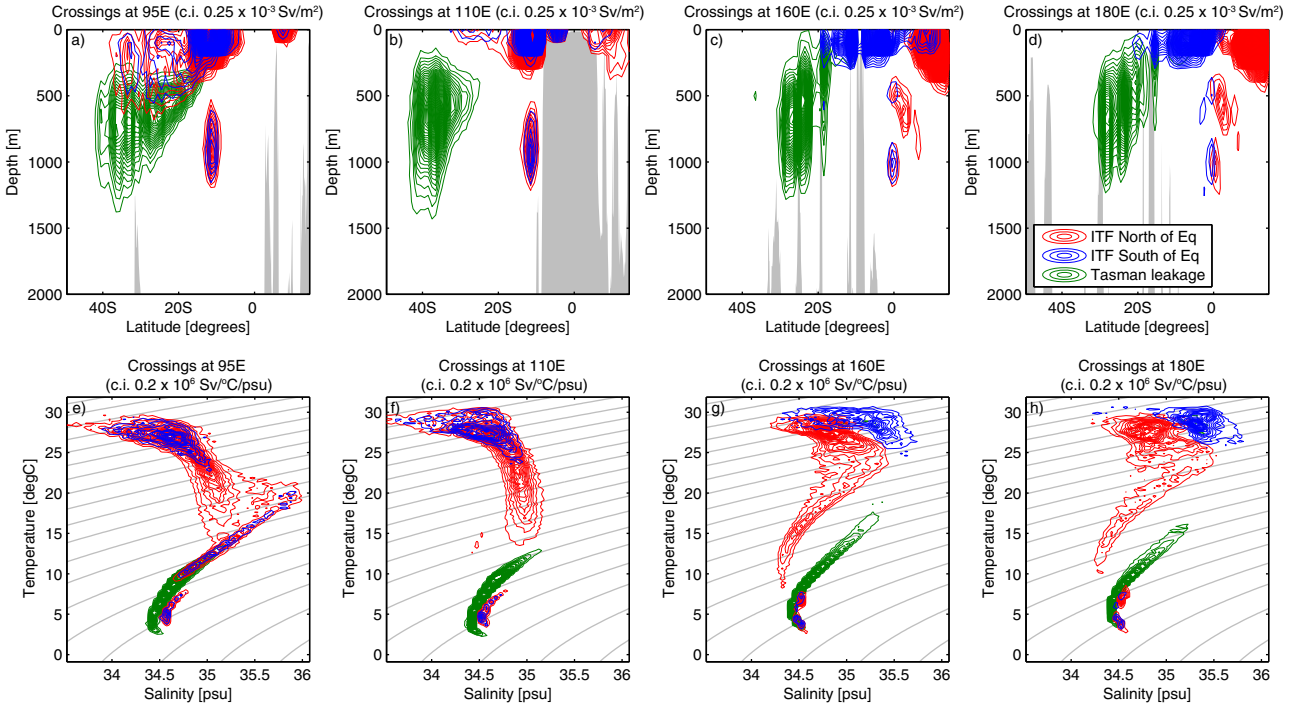

Figure 3. Crossing of particles at four different longitudes (95°E, 110°E, 160°E, and 180°E) in both depth-latitude (upper row) and temperature-salinity (lower row) space. Contours of the probability density function are drawn for three different particles: Tasman leakage in green, Indonesian Throughflow originating south of the Equator in blue, and Indonesian Throughflow originating north of the Equator in red. Contour intervals are 1 mSv/m^2 for the depth-latitude space and 0.2 × 10^6 Sv/°C/psu for the salinity-temperature space.

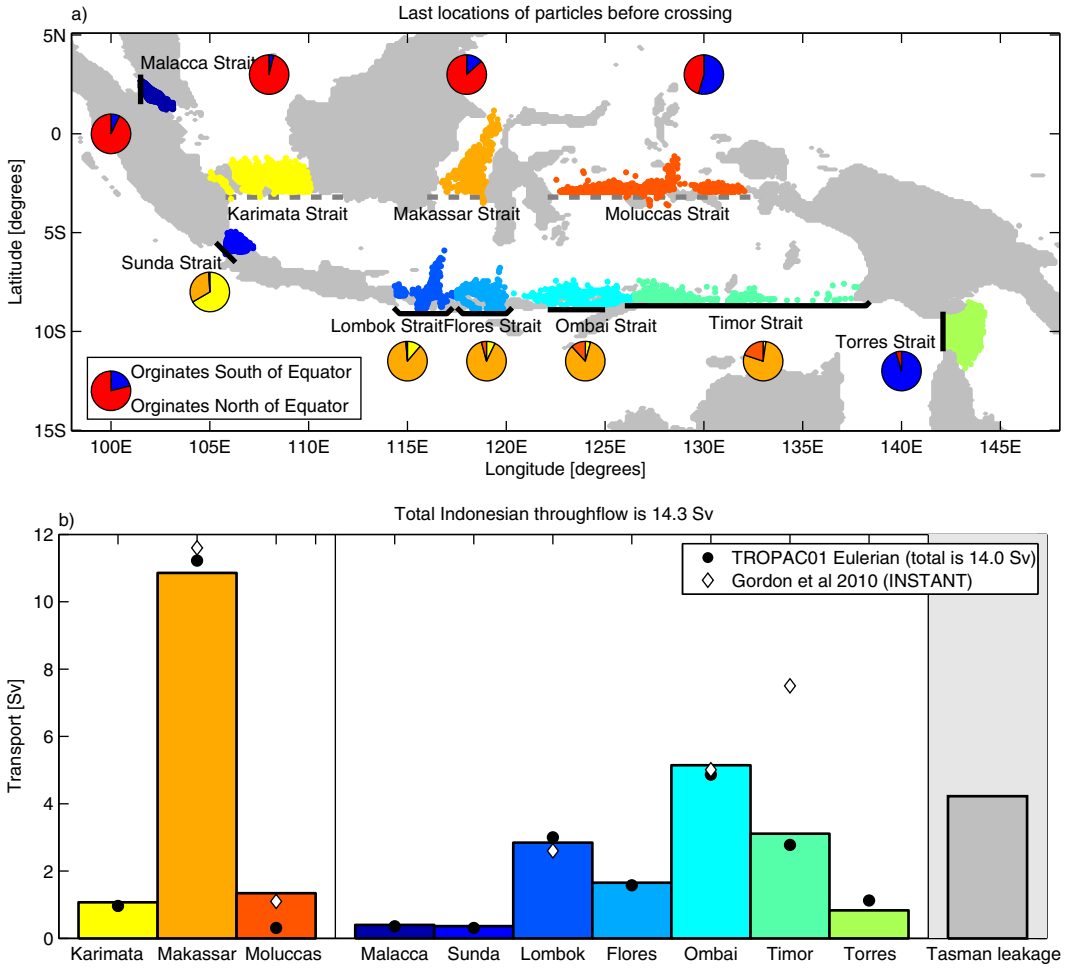

Figure 4. (a) The locations where particles that form the Indonesian Throughflow cross the different seas and straits in and out of the Indonesian Archipelago. The black lines are the lines used to separate Indian from Pacific Ocean in the conditional pathways. The dashed gray lines are the inflow lines. Note that for each crossing, only 1000 randomly selected particles are shown. The pie charts next to each strait depict the origin of the particles crossing there, either by hemisphere where they started in the Pacific (red/blue) or by which of the three inflow straits they came through (yellow-orange). (b) The total transport through each of the straits as measured by the Lagrangian particles. The black dots show the model Eulerian transports through the straits. The white markers show the observational estimates from the INSTANT observational program.

and backward in time. Again, the particles are assigned a transport equal to the local velocity in the grid cell times the area of that grid cell. This experiment is equivalent to the one undertaken by *van Sebille et al.* [2012] using velocity data from the Japanese OFES model.

2.3. Measuring Pacific-to-Indian Leakage Through Conditional Pathways

In total, almost 9 million particles are released and tracked in the TROPAC01 output across the two experiments. Most of these particles, however, do not reach the Indian Ocean. The analysis presented here is therefore undertaken using only a subset of the total particles released.

For the Indonesian Throughflow, only the particles that cross through the Indonesian Archipelago when tracked forward in time are selected, with the additional constraint that they reach one of the Indian Ocean domain boundaries before 31 December 2009. In the Indonesian Archipelago, the Pacific-Indian boundary is defined by the black lines between straits shown in Figure 4a. Out of the 8.0×10^6 particles released, 2.5×10^5 (~3%) particles satisfy these conditions. Furthermore, we divide the particles that form the Indonesian Throughflow into a subset of particles that start north of the Equator, and a subset of particles that start south of the Equator at 171°W.

For the Tasman leakage particles that are released south of Tasmania along the 146°E meridian, only particles that originate from the Pacific Ocean north of 35°S when tracked backward in time and also reach the

Indian Ocean north of 35°S when tracked forward in time are selected. This is the same definition as used in *van Sebille et al*. [2012]. Out of the 9.5×10^5 particles released, 8.8×10^4 (∼9%) particles satisfy these conditions.

The pathways of the particles selected in this way are *conditional pathways* [e.g., *van Sebille et al*., 2013] and it is the ability to query the full set of particle trajectories for these conditionals that makes Lagrangian analysis of ocean model data so useful. In the case of the Tasman leakage, for instance, the Lagrangian framework allows to select only that fraction of the flow that starts in the Pacific Ocean, rounds Tasmania and then ends in the Indian Ocean. Note that the conditions can be made even more complicated, including for instance constraints on the pathway depths, or constraints on the water mass properties following the particles (e.g., the in situ temperature and salinity along the particle trajectories). In this study, however, our goal is to understand sources and the partitioning of the transport via either the pathway north or south of Australia, and thus the conditions on the pathways described above are sufficient to investigate these issues.

3. Results

3.1. Basin-Scale Particle Pathways and Water Properties

The best way to appreciate the pathways of all interocean exchange particles is by watching an animation of them. This is available as supporting information or can be downloaded from https://dl.dropboxusercontent.com/u/8236298/ITFvsTL.avi. The animation clearly shows vigorous eddy variability in the particle trajectories, but also that there are some coherent pathways taken by large numbers of particles.

Maps of the long-term mean depth-integrated transport (in Sv/m^2) carried by particles passing through each $0.5^\circ \times 0.5^\circ$ grid cell summarize the pathways of all particles (Figure 2). This map is constructed by, for each grid cell, creating a map of which grid cells a particle visits on its journey from the green release line to the red end line. These binary maps of individual trajectories (1 if it visits a grid cell, 0 if not) are then multiplied by the transport carried by each particle, and all maps are added to one single map that essentially shows the transports of all particles that enter that grid cell. Finally, the map is normalized to the number of days on which particles are released. Importantly, this quantity is independent of how long a particle actually stays within a grid cell. Grid cells where more particles cross get a higher transport value and show up as stronger currents. This diagnostic clearly identifies the different origins and fates of the two interocean leakages.

Most particles that form the Indonesian Throughflow (Figure 2a) flow via the North Equatorial Current around 10°N in the Pacific Ocean, pass through the Indonesian Archipelago (see also section 3.2) and then enter the Indian Ocean at around 10°S–13°S. From there, most particles continue on a zonal path, although there appears to be considerable recirculation along this zonal path (see also the supporting information movie).

Some of the Indonesian Throughflow feeds into the Leeuwin Current (Figure 2a) and makes it all the way into the Great Australian Bight along the southern coast of Australia. However, most of the particles that reach the Bight recirculate and end up within the tropical Indian Ocean, so that ultimately very little of the Indonesian Throughflow connects back to the Pacific east of Tasmania on the time scales considered. These pathways agree well with those produced by *Valsala and Ikeda* [2007] and *Valsala et al*. [2011], who used Lagrangian particles in ocean models of lower spatial resolution to study the pathways of Indonesian Throughflow in both the Indian and Pacific Oceans.

The pathway for Tasman leakage is, in comparison, much more confined to subtropical and subpolar latitudes (Figure 2b). Most of the particles in the southern interocean exchange originate from the subtropical westward-flowing South Caledonian Jet arm of the South Equatorial Current between 20°S and 30°S. After reaching the Australian coast, the particles are advected southward with the East Australian Current and into the Tasman Sea eddy corridor [*Everett et al*., 2012]. Once the particles have rounded Tasmania, they flow on a relatively straight path to Cape Leeuwin, the southwestern most point of Australia. There is some recirculation around Cape Leeuwin, but in the end most of the Tasman leakage crosses 91°E south of 20°S (Figure 2b).

In longitude-latitude space (Figure 2), the pathways of the Indonesian Throughflow and the Tasman leakage seem to overlap in the southeast Indian Ocean. This is an aliasing artifact, however, as the pathways occupy

different depth ranges and so are not, per se, traversing the same water masses. This is clearly revealed in a series of depth-latitude cross sections (Figure 3). In the Indian Ocean at 95°E and 110°E (Figures 3a and 3b), two separate cores of the Indonesian Throughflow can be seen at 10°S. The largest core is found in the upper 300 m and a smaller core is found between 600 and 1200 m. These cores are consistent with the separation of the Indonesian surface water from the deeper Indonesian Intermediate water as found by *Talley and Sprintall* [2005]. In the eastern Indian Ocean, the Tasman leakage flow is mainly confined south of 15°S, and between 300 and 1100 m. This deep Tasman leakage pathway carrying intermediate water has recently been confirmed in Argo data [*Rosell-Fieschi et al*., 2013].

All particles that pass through the Indonesian Archipelago in the Indonesian Throughflow can be further subdivided into particles that originate north of the equator (70% of the total Indonesian Throughflow, red in Figure 3a) and particles that originate south of the equator (30% of Indonesian Throughflow, blue in Figure 3a) at 171°W. There has been debate in the past as to how much of the Indonesian Throughflow originates from the South Pacific [*Godfrey et al*., 1993; *Gordon*, 1995], and better characterization of the sources of the Indonesian Throughflow can help in understanding its role in the global ocean circulation. The Lagrangian particles provide a unique opportunity to address some of these questions within the model framework.

In the Indian Ocean, both the deep and shallow cores of the Indonesian Throughflow at ∼10°S appear well mixed with waters of North and South Pacific origin (Figures 3a and 3b). Moving upstream into the Pacific Ocean (Figures 3c and 3d), however, the waters from the different hemispheres occur in two essentially unconnected cores above 400 m. Note, however, that this is partly by construction, as the conditional pathways for North Pacific Indonesian Throughflow requires those particles originate either across 14°N or across 171°W north of the Equator.

There is also a small core of deeper Indonesian Throughflow water (around 500 m) in the Pacific Ocean that is almost exclusively of North Pacific origin, but this core is both weaker and shallower than the deep core in the Indian Ocean. Deeper cores of mixed North and South Pacific waters occur at ∼1000 m depth in the Pacific sections, although their transport contribution is minor (<1 mSv/m^2). That this deeper transport core is enhanced and becomes apparent in the Indian Ocean sections (Figures 3a and 3b), supports the occurrence of vigorous mixing in the internal seas to produce this water mass [*Ffield and Gordon*, 1996; *Hautala et al*., 1996; *Talley and Sprintall*, 2005].

At each of the four zonal sections, the particle crossings can also be plotted in temperature-salinity space (Figures 3e–3h). In the Indian Ocean, most of the Indonesian Throughflow water is well mixed in the thermocline and deep cores, but there is a water mass (between 15°C. and 25°C, with a narrow salinity range centered on ∼35) that is almost exclusively of North Pacific origin. At 95°E, a distinct tail of mixed Indonesian Throughflow water occurs roughly along the same isopycnal as the Tasman Leakage waters (Figure 3e) although slightly warmer and saltier.

In the Pacific Ocean (Figures 3g and 3h), the South Pacific thermocline water is much more saline than the North Pacific water. Comparing the properties of the Indonesian Throughflow water at 180°E to those at 160°E, as noted above, some of the mixing of Indonesian Throughflow appears to have occurred in the western Equatorial Pacific. However, in the shallower core, mixing within the Indonesian Seas has clearly eroded the Pacific stratification of the salinity maximum associated with the North Pacific Subtropical water mass (Figures 3e–3h). In the Indian Ocean sections, the surface layer is much fresher compared to the Pacific sections (Figures 3e–3h), reflecting the voluminous input of freshwater and mixing within the internal Indonesian Seas.

The Tasman leakage is much colder than most of the Indonesian Throughflow, although the coldest Tasman leakage is as cold but slightly fresher than the deep Intermediate core of the Indonesian Throughflow water. Since almost all Tasman leakage is carried below 300 m depth, its TS signature is rather narrow. Remote from the surface, the Tasman leakage goes through little water mass conversion compared to the Indonesian Throughflow as it flows from 180°E to 95°E, becoming slightly fresher but maintaining a tight TS relationship. Note that in the salinity minimum at depth in the Indian Ocean sections, there is clear separation of the fresher Antarctic Intermediate water component of the Tasman leakage from the (comparatively) saltier Indonesian Intermediate water, as also found in observations [*Talley and Sprintall*, 2005].

3.2. Particle Connectivity in the Indonesian Archipelago

A more detailed investigation of the pathways of Indonesian Throughflow particles in the Indonesian Archipelago is shown in Figure 4. This figure shows—for each of the 10 main inflow and outflow straits—how much transport crosses that strait and where the particles originate. Most of the inflow into the Java/Banda Sea region goes through Makassar Strait (10.9 Sv, Figure 4b), which is slightly lower than observed estimates of 11.6 Sv reported by *Gordon et al*. [2010] from the 3 year INSTANT mooring program and the 13.3 Sv [*Susanto et al*., 2012] for the extended mooring period until 2011. The observational and model estimates are still consistent, however, in that there are 3 year periods in the TROPAC01 output when the Makassar Strait transport is larger than 12.5 Sv.

In addition to the 10.9 Sv entering the Indonesian Seas through Makassar Strait, another $\sim$1 Sv enters the region between Sumatra and Kalimantan (here referred to as the Karimata Strait, although it is a collection of straits) as well as through the region between Sulawesi and the Maluku Islands (here referred to as the Moluccas Strait). Most of the water through Karimata Strait is of Northern Pacific origin, with a slightly larger proportion of South Pacific water going through Makassar Strait. In the Moluccas Strait, on the other hand, just over half of the water is of South Pacific origin.

The outflow from the Java Sea/Banda Sea region into the Indian Ocean is more evenly divided between the different straits than the inflow (Figure 4b). Ombai Strait carries the largest transport of Indonesian Throughflow particles (5.1 Sv or 36%), with Timor and Lombok Straits both carrying $\sim$3 Sv. For all straits except Sunda, the main contribution comes from Makassar Strait (Figure 4a). In general, the proportion of water coming from the Moluccas Strait decreases going west and the proportion of water coming from Karimata Strait decreases going east, with distance from the source.

Not all Indonesian Throughflow water passes through the Java and Banda Seas. Some particles cross either Malacca Strait or Torres Strait. The former strait carries water almost exclusively of North Pacific origin via the South China Sea, while the latter strait carries water almost purely from the South Pacific.

The temperature-salinity profile of the water as it crosses the most important inflow and outflow straits (Figure 5) reveals that most of the deep and cold water enters the Indonesian Seas through Moluccas Strait (i.e., 95% of the water colder than 10°C, Figure 5c). This cold water then flows out of the Indonesian Seas mainly through Timor Strait (71% of the water colder than 10°C, Figure 5g), with the rest passing through Ombai Strait (Figure 5f). Note that, compared to the water masses in the Indian and Pacific Oceans (Figure 3), the subsurface water in the outflow straits (colder than 25°C) have very uniform salinity, in agreement with the observations from *Talley and Sprintall* [2005].

Closer to the surface, it is interesting that in all straits, except in Karimata, a significant fraction of the warm ($>$25°C) and relatively saline (between 34 and 35 psu) water is of Southern Hemisphere origin. This is even true in Lombok and Flores Straits, which receive this Southern Hemisphere water from Makassar Strait. Also clear from Figure 5 is that most of the freshest water enters the Indonesian Seas through Karimata Strait (71% of the water fresher than 33.2 psu, Figure 5a) and then exits through Lombok Strait (58% of the water fresher than 33.2 psu, Figure 5d). This water is largely (88%) of Northern Hemisphere origin.

The connectivity between the different straits around the Indonesian Seas, partitioned into water of Southern and Northern Hemisphere origin, is shown in Figure 6. This shows that more water of Southern Hemisphere origin flows into the Indonesian Seas through Makassar Strait than through Moluccas Strait. Makassar Strait contributes at least 0.1 Sv to all outflow straits, with the largest connection between Makassar and Ombai Straits (4.3 Sv). The other two inflow Straits, on the other hand, do not contribute $>$0.1 Sv to all outflow straits, so their connectivity is limited. It is worth noting that such an analysis of the connectivity between inflow and outflow straits can only be done in a Lagrangian framework, and this is the first time it has been done for the Indonesian Throughflow within an eddy-resolving model.

The total Indonesian Throughflow from the Lagrangian particles in this model is 14.3 Sv, which is in very good agreement with the net outflow of 15 Sv found during the 3 year INSTANT observational program [*Sprintall et al*., 2009; *Gordon et al*., 2010]. In most of the individual straits, the Lagrangian transports in TROPAC01 agree very well with the observational estimates from INSTANT (Figure 4b), as reported in *Gordon et al*. [2010]. The only exception to this is the transport through Timor Strait, which is 7.5 Sv in the observations and slightly $>$3 Sv in the model. Part of this discrepancy can be attributed to the fact that the Timor

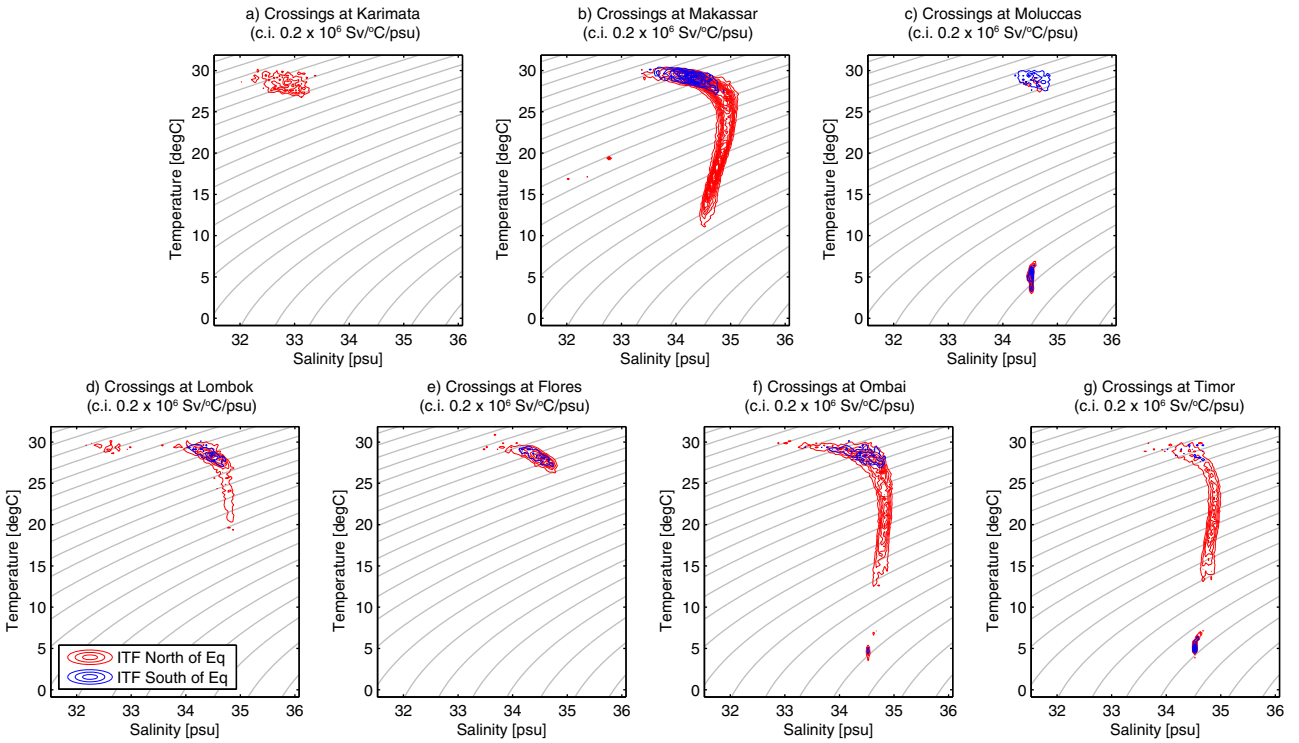

Figure 5. (a–c) Crossing of particles through the most important inflow and (d–g) outflow straits in temperature-salinity space. Contours of the probability density function of Indonesian Throughflow waters originating from south of the Equator are drawn in blue and for particles originating north of the equator are drawn in red. Contour intervals are 0.2 × 10^6 Sv/°C/psu for the salinity-temperature space.

Strait was defined differently in INSTANT: in that observational program it is based on a meridional section between Timor and Australia, and so this also incorporates Torres Strait water. But even combining the simulated flow through the Timor and Torres Straits, the observed value is ∼2 Sv higher than that using either Eulerian or Lagrangian model estimates. It is also unlikely that interannual variability can explain the discrepancy between model and observation, as there is no 3 year period in TROPAC01 where the combined Timor and Torres Strait transport reaches the observed 7 Sv (the maximum in TROPAC01 is 4.8 Sv). Hence, we must conclude that this discrepancy between Timor Strait transport in model and observations is likely to be either due to a bias in TROPAC01 and/or an issue with the observations. In support of the latter possibility, it is worth noting that *Molcard et al.* [1996] found a Timor Strait transport of only 4.3 Sv, which is much closer to the TROPAC01 model results than the INSTANT value.

The Indonesian Throughflow is on average unidirectional (almost always from the Pacific to the Indian Ocean) and mostly confined from the upper to intermediate depths. Unlike the Tasman leakage or Agulhas leakage for instance, these properties mean that the Lagrangian and Eulerian estimates of the Indonesian Throughflow can directly be compared. This enables assessment of whether the methods used in large-scale Lagrangian experiments such as this one are reasonable, whereby particles are assigned a transport as they are released and that transport is then conserved along the particle pathway.

The Lagrangian estimates agree well with the Eulerian fluxes through the inflow and outflow straits calculated from the local velocities (Figure 4b, bars versus black circles). The sum of Eulerian transports (14.0 Sv) is only slightly smaller than that of the Lagrangian transport (14.3 Sv). This is despite the fact that in principle they measure quite different quantities. The Lagrangian particles measure only the transport by water parcels that start at either 14°N or 171°W and end at 91°E. The good agreement between Lagrangian and Eulerian transports suggests that other sources of water in the Indonesian Throughflow, particularly from the Southern Ocean, play a negligible role.

In almost all straits, the Lagrangian and Eulerian estimates agree to within 0.3 Sv (Figure 4b). The only exception to this is Moluccas Strait, where the Eulerian transport is 1.0 Sv smaller than the Lagrangian

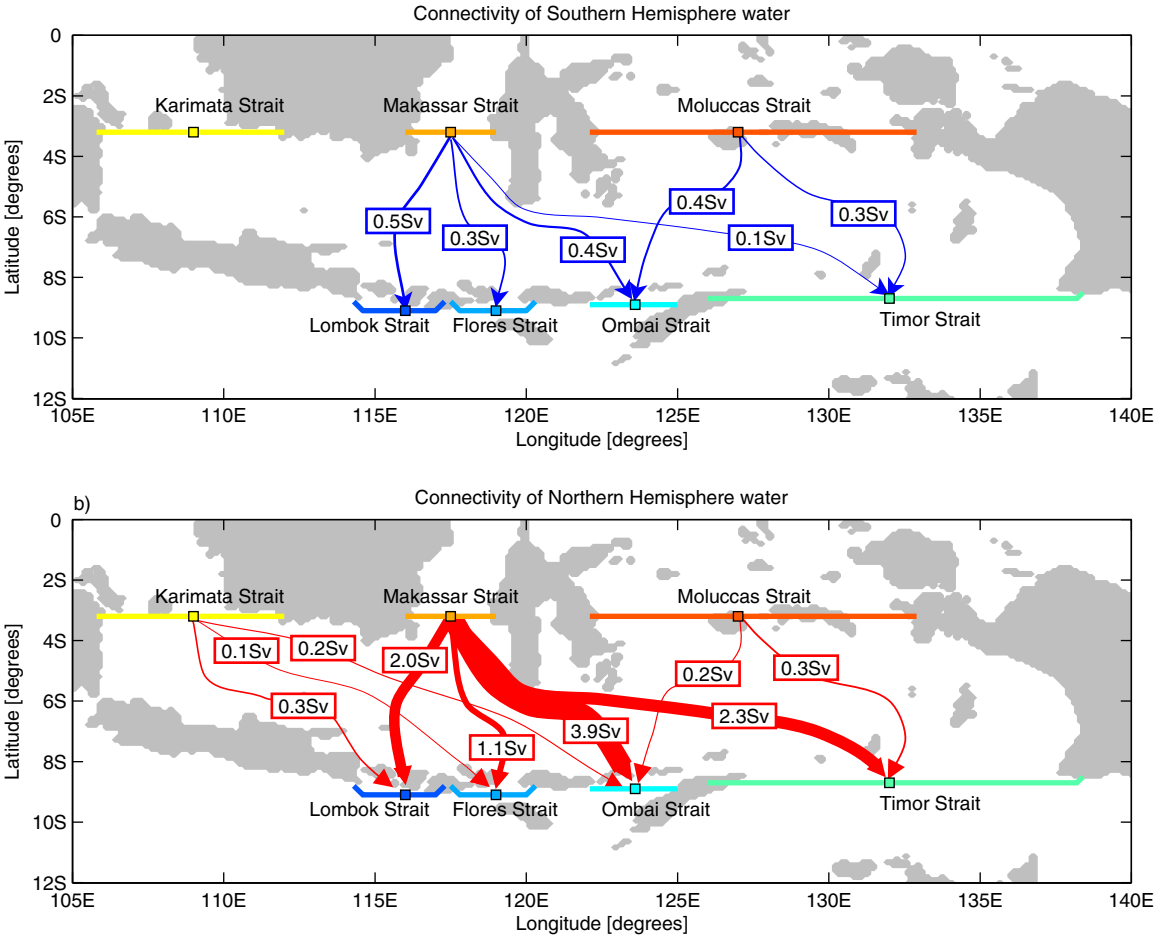

Figure 6. Connectivity between the straits flowing into and out of the Indonesian Seas, for both water of (a) Southern Hemisphere origin and (b) Northern Hemisphere origin. Transports are given in Sv and transports lower than 0.1 Sv are not shown.

transport. It is unclear why the Lagrangian transport is so much larger in Moluccas Strait, especially because the reason given above as to why Eulerian and Lagrangian transports might not agree would imply that the Lagrangian transport should be biased low. In any case, the convergence of flow through the Banda and Java Seas (inflow minus outflow) is 0.0 Sv in the Eulerian estimates and +0.2 Sv in the Lagrangian case, explaining only a fraction of the 1.0 Sv discrepancy in Moluccas Strait. The relatively poor agreement between Eulerian and Lagrangian transports in Moluccas Strait is therefore not explained, but given the good agreement between the two measures of transport in all other straits, we are confident in the fidelity of the Lagrangian approach used here.

3.3. Time Series of Tasman Leakage and Indonesian Throughflow

As yet we have only discussed results based on time-averaged transports. However, the Lagrangian framework also allows for calculation of time-varying interocean exchanges, as we know the date that each particle crosses from the Pacific into the Indian Ocean. One drawback of the Lagrangian method, however, is that it suffers from a ramp-up and ramp-down effect [*van Sebille et al.*, 2012]. This is because it takes time for particles to get from the Pacific Ocean release sections to the Indian Ocean (Figure 7). The length of the ramp-up effect depends on the route the water takes, and is much shorter in the fast-flowing tropical Pacific than in the route around Tasmania. Similarly, there is also a ramp-down effect because it takes time for particles to travel from the Pacific-Indian boundary to the end line at 91°E (for the Indonesian Throughflow) or 35°S (for the Tasman leakage).

Comparison to the Eulerian time series leads to estimates that the ramp-up of the Indonesian Throughflow takes ~3 years, while its ramp-down takes ~7 years (Figure 7). The particles that cross the Indonesian

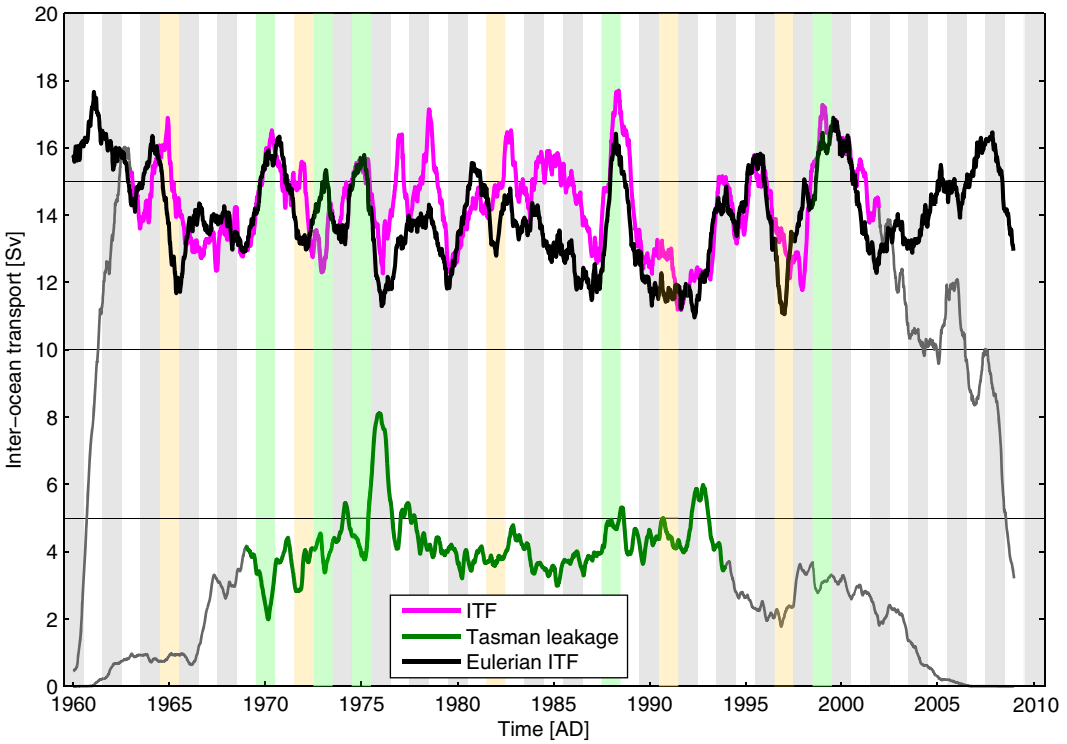

Figure 7. Time series of Lagrangian Indonesian Throughflow (in purple) and Tasman leakage (in green), as well as that of the Eulerian Indonesian Throughflow (in black). In all cases, a 1 year moving-average smoothing window has been applied. Yellow bars denote the El Niño years used in Figures 8 and 9, while green bars denote the La Niña years. The Lagrangian time series have a ramp-up and ramp-down effect (gray lines at beginning and end of each time series) as it takes particles time to reach the crossing sections from their start and end sections (see also the text).

Throughflow within these 10 years (the gray lines in Figure 7) have not been used in any of the analyses presented in this study. Just as in the time-mean transports through the individual straits (Figure 4), the agreement between the Eulerian and Lagrangian Indonesian Throughflow is very good, with most of the interannual variability captured (Figure 7). The temporal correlation between the Lagrangian and Eulerian time series of the Indonesian Throughflow for the 39 remaining years is $R = 0.64$, which is significant at the 95% confidence level.

In both the Lagrangian and in particular the Eulerian time series of Indonesian Throughflow, there is the suggestion of two different multidecadal trends. As already reported by *Feng et al*. [2011], the Indonesian Throughflow seems to steadily decrease until 1993, after which it increased again. Given that the forcing used in the TROPAC01 model is based on the same reanalysis products as used by this previous study, this result is somewhat to be expected.

The Tasman leakage is smaller than the Indonesian Throughflow, but not insignificant. As there is no Eulerian time series to compare with, the ramp-up and ramp-down time scales are determined using the time it takes 90% of the particles to reach the Pacific Ocean when tracked backward and the time scale it takes 90% of the particles to reach the Indian Ocean when tracked forward, respectively [see also *van Sebille et al*., 2012]. This leads to a ramp-up time scale of 9 years and a ramp-down time scale of 15 years. The mean value of Tasman leakage in TROPAC01 is 4.2 Sv, which happens to be exactly the same as the mean in the OFES model [*van Sebille et al*., 2012].

3.4. Interannual Variability in Indian-Pacific Exchange and its Relation to ENSO

The interannual variability in Tasman leakage is clearly smaller than that in Indonesian Throughflow (Figure 7). The most obvious signal in Tasman leakage is the large spike in 1976, which coincides with a local minimum in the 50 year Indonesian Throughflow time series. The lagged cross correlation between the two time series on 5 day temporal resolution and smoothed with a 1 year running-mean window, however, does not reveal any statistically significant relationship (not shown). There are two peaks in the cross

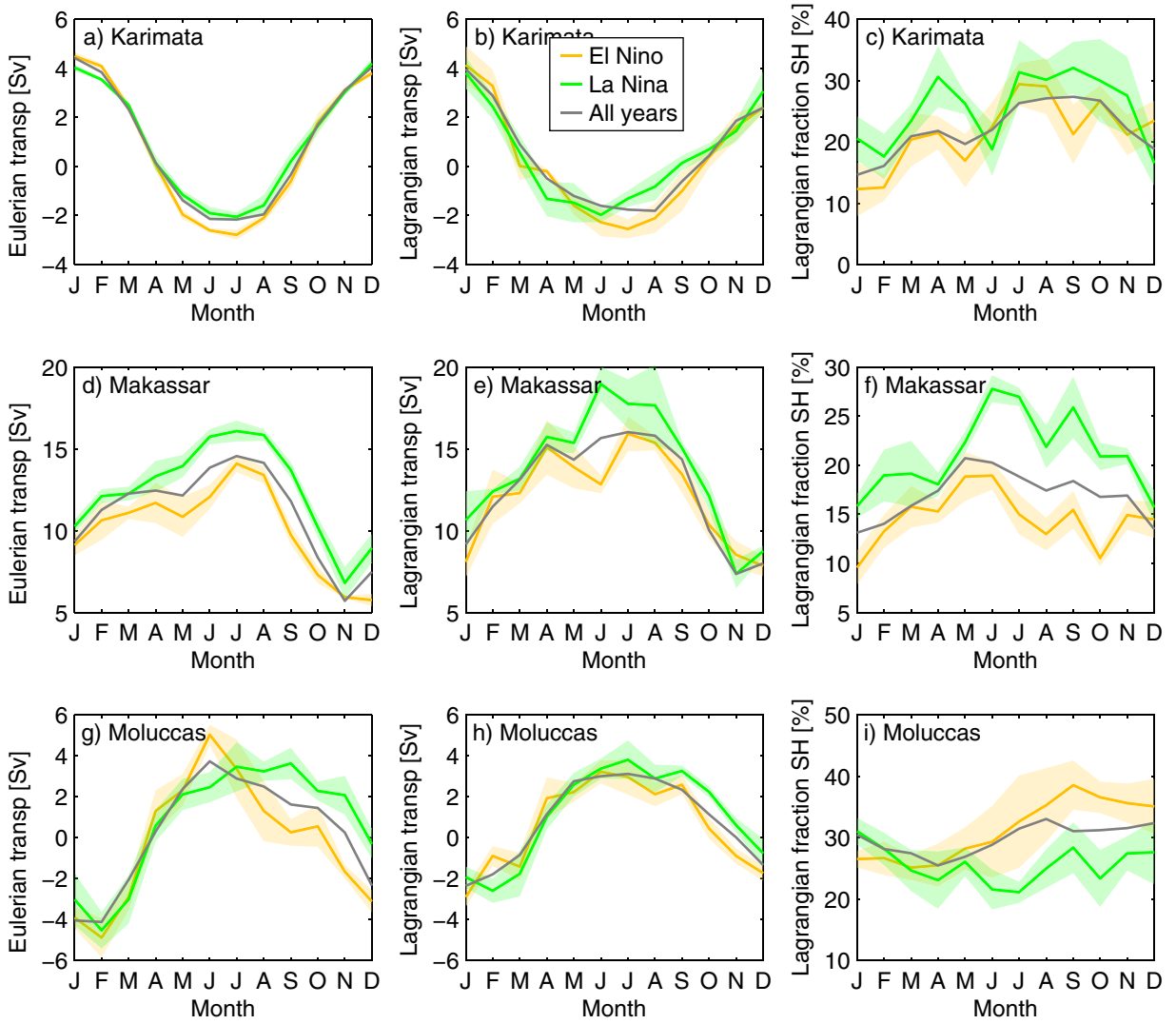

Figure 8. (left) The Eulerian and (middle) Lagrangian transports, as well as the particle-derived fractions of transport originating from the (right) Southern Hemisphere at 171W through each of the three Indonesian inflow straits for the year of each El Niño (orange) and La Niña (green) event (see also Figure 7). The envelopes represent standard error based on the five different events considered. The gray lines show the annual cycle of transports and fractions. (d and e) Most notably is the 1–2 Sv peak in Makassar Strait transports in June/July leading up to La Niña events, mirrored by a similar reduction for El Niño events. (f) Most of this variability can be attributed to changes in the amount of water from the Southern Hemisphere.

correlation between the Lagrangian Tasman leakage and the Lagrangian Indonesian Throughflow: one with a correlation of −0.26 where the Tasman leakage leads the Indonesian Throughflow by 3 months and one with a correlation of −0.40 where the Tasman leakage leads the Indonesian Throughflow by almost 16 years. However, neither of these correlations is significant at even the 80% confidence level. We must therefore conclude that, if there is any compensation or covariation between the transports through the two Pacific-to-Indian pathways in this model, it is occurring on decadal or longer time scales.

As previous studies have also shown [*Meyers*, 1996; *England and Huang*, 2005], the Indonesian Throughflow transport is correlated to ENSO: typically, the transport is stronger during La Niña years and weaker during El Niño years. Although this relationship is not perfect (there are non-ENSO years when transport peaks and similarly ENSO years when transport is relatively average, see also Figure 7), part of the interannual variability in Indonesian Throughflow in TROPAC01 can be related to NINO34 variability. The maximum correlation between the monthly binned, full-depth Eulerian time series (black line in Figure 7) and the NINO34 index (sea surface temperature anomaly averaged in the region 5°N–5°S, from 170°W to 120°W) is $R = -0.61$, significant at the 95% confidence level, when the Indonesian Throughflow leads NINO34 by 3 months. The corresponding correlation for the monthly binned, full-depth Lagrangian time series (purple line in Figure 7) at

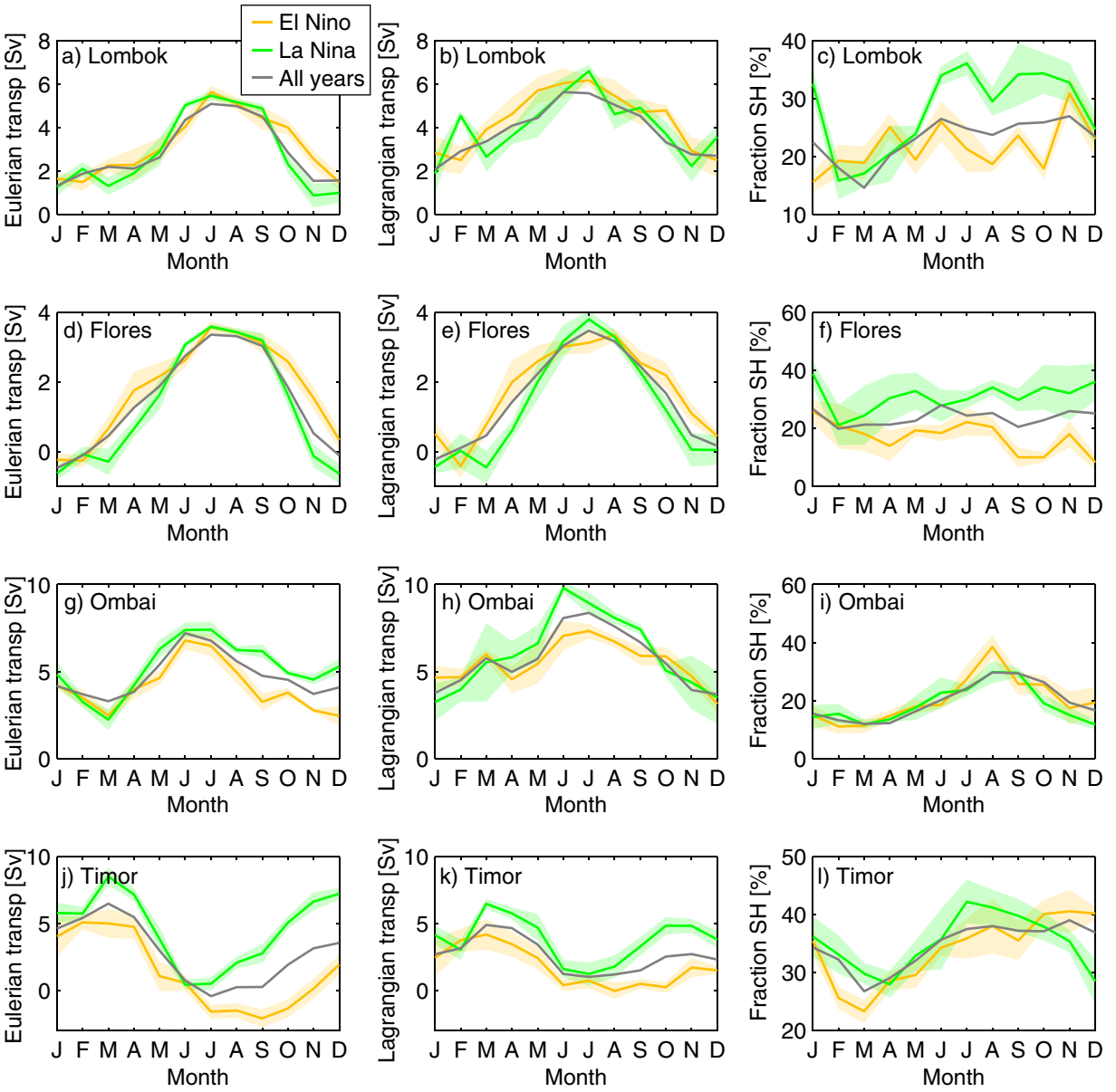

Figure 9. (left) The Eulerian and (middle) Lagrangian transports, as well as the particle-derived fractions of transport originating from the (right) Southern Hemisphere at 171W through four main Indonesian outflow straits for the year of each El Niño (orange) and La Niña (green) event (see also Figure 7). The envelopes represent standard error based on the five different events considered. The gray lines show the annual cycle of transports and fractions. See also Figure 8.

the 3 month lead is −0.41, which is also significant, but the maximum correlation is $R = -0.54$ when the Indonesian Throughflow lags NINO34 by 2 months. Despite the slight time-lag difference between the two approaches, the Lagrangian particles do capture the overall Eulerian features in terms of seasonal cycle and the contrast between El Niño and La Niña, as demonstrated below.

Figure 8 presents the monthly Indonesian Throughflow transport at each of the three main inflow straits composited over the five strongest El Niños (1965, 1972, 1982, 1991, and 1997) and La Niñas (1970, 1973, 1975, 1988, and 1999). The composites, which also show the proportion of waters that come from the South Pacific (right plots), span the developing year of ENSO, which typically begins during boreal spring in April to May and peaks around December. The seasonal cycle of the transports based on the Eulerian and Lagrangian estimates are in good agreement with each other and with the observations. The Makassar transport (Figure 8, middle) peaks around boreal summer and is lowest in boreal winter due to strong monsoon influence [*Gordon et al.*, 1999, 2008]. A similar seasonal cycle is exhibited by the Moluccas transport, supporting

the results of *Du and Qu* [2010] based on SODA reanalysis. An out-of-phase seasonal evolution is seen in the Karimata transport, with a maximum in boreal winter and reversed flow in boreal summer, consistent with recent observations in this strait [*Fang et al*., 2010; *Susanto et al*., 2013].

Across the three inflow straits (Figure 8), transports are larger during La Niña. However, the most striking difference is seen in the transport through the Makassar Strait in boreal summer during which ENSO events develop (Figures 8d and 8e). The portion of hemispheric water source according to ENSO phases is also most markedly different in this strait (Figure 8f), with a significantly greater amount of water coming from the Southern Pacific during La Niña. This appears consistent with the idea that even though the Indonesian Throughflow appears to be sourced from the North Pacific it is partly fed by South Pacific waters via the South Equatorial Current and via the New Guinea Coastal Current system [*Godfrey et al*., 1993]. While some South Pacific waters may directly pass into the Indonesian Seas, the remainder ends up in the North Pacific through recirculation in the North Equatorial Counter Current and North Equatorial Current, eventually feeding the Indonesian Throughflow via the Mindanao Current. Thus, during La Niña the South Pacific water portion is expected to be enhanced as shown in Figure 8 (right). In addition, recent results suggest that during La Niña events, inflow to the Indonesian Throughflow via the South China Sea is reduced and hence permits a more direct inflow from the Pacific [*Gordon et al*., 2012].

The ENSO associated change in the portion of South Pacific waters for the Moluccas Strait is opposite to that for the Makassar, with a larger amount of South Pacific waters during El Niño. This is consistent with previous studies [e.g., *Valsala et al*., 2011]. On the other hand, there is less discernible ENSO effect through the Karimata Strait (Figures 8a and 8b). The intraseasonal oscillations in the percent contribution from the South Pacific in Karimata Strait (Figure 8b) might be interpreted as a response to elevated Madden-Julian Oscillation activity during La Nina events that result in pulses of Pacific water entering the South China Sea and subsequently into Karimata Strait.

Figure 9 shows the ENSO-induced transport changes through the four most important outflow straits. Certain straits, such as Lombok and Flores show larger transport during El Niño, while Ombai and Timor show larger transport during La Niña. Given the paucity of long-term observational data at present in these passages, a one-to-one comparison with observations is not as yet possible. Nonetheless, our results paint a complex picture for the partitioning of ENSO-induced transports through the outflow straits. Further studies using different models are needed to examine this issue in more detail.

4. Conclusions and Discussion

We have tracked virtual Lagrangian particles in the high-resolution TROPAC01 model covering the circum-Australian oceans to study the pathways and transport variability of the Indonesian Throughflow and Tasman leakage. Although the flow through the Indonesian Archipelago carries 3.5 times more water from the Pacific into the Indian Ocean than the flow around Tasmania, both are likely important for global climate. The two routes carry quite different water masses, with the Tasman leakage almost exclusively below the mixed layer and of subtropical origin. The Indonesian Throughflow is primarily confined to the upper 300 m and of tropical origin, and has a separate deeper core at $\sim$1000 m consisting of intermediate water.

Given that their sources are so different, it is perhaps of little surprise that no statistically significant relationship was found between the time series of Tasman leakage and Indonesian Throughflow. As also discussed in section 1, one possible hypothesis that might suggest a relationship between Indonesian Throughflow and Tasman leakage variability is that both originate in the tropical Pacific and that the bifurcation of the South Equatorial Current in the Coral Sea would determine the distribution between northward and southward flows. The analysis presented here, however, suggests that this is not the case and that this hypothesis is false on the time scales considered here. Almost all Tasman leakage originates from further south and from much deeper sources than even the southernmost component of the Indonesian Throughflow. Note, however, that it could still be possible that the two pathways compensate on much longer (centennial to millennial) time scales, driven by the global large-scale wind and buoyancy patterns.

Within the Indonesian Archipelago, the virtual Lagrangian particles provide a unique picture of the connectivity between the different inflow and outflow straits. Most of the Indonesian Throughflow originates in the North Pacific Ocean, and only in the eastern passageways of Moluccas and Torres Straits is the bulk of the

water of South Pacific origin. Within the model, the distributions of source regions change between El Niño and La Niña years, in line with the observed enhanced transport during La Niña [*Meyers*, 1996], but the overall effect of ENSO on the connectivity between the inflow and outflow straits is rather limited. The relation is also much more complicated than earlier studies have identified by looking at the relation between ENSO and the Indonesian Throughflow as a whole [*Meyers*, 1996; *England and Huang*, 2005] suggested. While transport decreases in some straits (Makassar, Karimata) in El Niño years, it increases during these years in other straits (Flores, Lombok to some extent). The timing of the response in transport to ENSO is also different for the straits, providing an additional explanation of why the previously observed correlation between ENSO and Indonesian Throughflow strength is so low.

The Indonesian Archipelago provides an ideal opportunity to validate the Lagrangian approach that has been used in many large-scale oceanography applications [*Döös*, 1995; *Speich et al*., 2002; *Biastoch et al*., 2009; *van Sebille et al*., 2009, 2012, 2013], where water parcels are tagged with a certain transport as they are released and are then assumed to maintain that transport along their trajectories. Even though the Lagrangian approach has drawbacks such as the ramp-up and ramp-down effects (as evident in Figure 7) it is at present the only viable way to infer complex interocean exchanges such as the Tasman leakage. Our results provide justification for this Lagrangian approach. The local Eulerian flow through the individual Indonesian Straits and the transport obtained from the Lagrangian particles are in very good agreement, as is the interannual variability in total transport.

As the ocean model used in this study is a subdomain of a regionally nested high-resolution model, it is beyond the scope of this study to investigate the fate of the Indonesian Throughflow in the Western Indian Ocean. Better understanding of the pathways from the individual Indonesian Passages to the Agulhas Current would be of great interest to the community studying the Agulhas system and the Indian-to-Atlantic interocean exchange, as the roles of the Tasman leakage and Indonesian Throughflow are active topics of research in this region [*Casal et al*., 2009; *Le Bars et al*., 2013].

Acknowledgments
This project was supported by the Australian Research Council via grants DE130101336 and FL100100214. J. S. was supported by the NASA Physical Oceanography award NNX13AO38G. TROPAC01 was developed within the framework of the DFG project SFB754 and integrated at the North-German Supercomputing Alliance (HLRN).

References

Aldrian, E., and R. D. Susanto (2003), Identification of three dominant rainfall regions within Indonesia and their relationship to sea surface temperature, *Int. J. Climatol.*, *23*(12), 1435–1452, doi:10.1002/joc.950.

Annamalai, H., S. Kida, and J. Hafner (2010), Potential impact of the Tropical Indian Ocean–Indonesian Seas on El Niño characteristics, *J. Clim.*, *23*(14), 3933–3952, doi:10.1175/2010JCLI3396.1.

Barnier, B., et al. (2006), Impact of partial steps and momentum advection schemes in a global ocean circulation model at eddy-permitting resolution, *Ocean Dyn.*, *56*(5–6), 543–567, doi:10.1007/s10236-006-0082-1.

Barnier, B., et al. (2007), Eddy-permitting ocean circulation hindcasts of past decades, *Clivar Exch.*, *12*, 8–10.

Biastoch, A., L. M. Beal, J. R. E. Lutjeharms, and T. G. D. Casal (2009), Variability and coherence of the Agulhas undercurrent in a high-resolution ocean general circulation model, *J. Phys. Oceanogr.*, *39*(10), 2417–2435, doi:10.1175/2009JPO4184.1.

Cai, W. (2006), Antarctic ozone depletion causes an intensification of the Southern Ocean super-gyre circulation, *Geophys. Res. Lett.*, *33*, L03712, doi:10.1029/2005GL024911.

Cai, W., A. Sullivan, and T. Cowan (2011), Interactions of ENSO, the IOD, and the SAM in CMIP3 Models, *J. Clim.*, *24*(6), 1688–1704, doi:10.1175/2010JCLI3744.1.

Casal, T. G. D., L. M. Beal, R. Lumpkin, and W. E. Johns (2009), Structure and downstream evolution of the Agulhas Current system during a quasi-synoptic survey in February-March 2003, *J. Geophys. Res.*, *114*, C03001, doi:10.1029/2008JC004954.

Debreu, L., C. Vouland, and E. Blayo (2008), AGRIF: Adaptive grid refinement in Fortran, *Comput. Geosci.*, *34*(1), 8–13, doi:10.1016/j.cageo.2007.01.009.

Döös, K. (1995), Interocean exchange of water masses, *J. Geophys. Res.*, *100*, 13,499–13,514.

Du, Y., and T. Qu (2010), Three inflow pathways of the Indonesian Throughflow as seen from the simple ocean data assimilation, *Dyn. Atmos. Oceans*, *50*(2), 233–256, doi:10.1016/j.dynatmoce.2010.04.001.

England, M. H., and F. Huang (2005), On the interannual variability of the Indonesian Throughflow and its linkage with ENSO, *J. Clim.*, *18*, 1435–1444.

England, M. H., C. C. Ummenhofer, and A. Santoso (2006), Interannual rainfall extremes over southwest Western Australia linked to Indian Ocean climate variability, *J. Clim.*, *19*(10), 1948–1969.

Everett, J. D., M. E. Baird, P. R. Oke, and I. M. Suthers (2012), An avenue of eddies: Quantifying the biophysical properties of mesoscale eddies in the Tasman Sea, *Geophys. Res. Lett.*, *39*, L16608, doi:10.1029/2012GL053091.

Fang, G., R. D. Susanto, S. Wirasantosa, F. Qiao, A. Supangat, B. Fan, Z. Wei, B. Sulistiyo, and S. Li (2010), Volume, heat, and freshwater transports from the South China Sea to Indonesian Seas in the boreal winter of 2007–2008, *J. Geophys. Res.*, *115*, C12020, doi:10.1029/2010JC006225.

Feng, M., C. Böning, A. Biastoch, E. Behrens, E. Weller, and Y. Masumoto (2011), The reversal of the multi-decadal trends of the equatorial Pacific easterly winds, and the Indonesian Throughflow and Leeuwin Current transports, *Geophys. Res. Lett.*, *38*, L11604, doi:10.1029/2011GL047291.

Ffield, A., and A. L. Gordon (1996), Tidal mixing signatures in the Indonesian Seas, *J. Phys. Oceanogr.*, *26*, 1924–1937.

Godfrey, J. S., A. C. Hirst, and J. Wilkin (1993), Why does the Indonesian Throughflow appear to originate from the North Pacific? *J. Phys. Oceanogr.*, *23*(6), 1087–1098.

Gordon, A. L. (1995), When is appearance reality? A comment on why does the Indonesian Throughflow appear to originate from the North Pacific, *J. Phys. Oceanogr.*, *25*, 1560–1567, doi:10.1175/1520-0485(1995)025<1560:WIARAC>2.0.CO;2.
Gordon, A. L. (2005), Oceanography of the Indonesian Seas and their Throughflow, *Oceanography*, *18*, 14–27.
Gordon, A. L., R. D. Susanto, and A. Ffield (1999), Throughflow within Makassar Strait, *Geophys. Res. Lett.*, *26*(21), 3325–3328.
Gordon, A. L., R. D. Susanto, A. Ffield, B. A. Huber, W. Pranowo, and S. Wirasantosa (2008), Makassar Strait Throughflow, 2004 to 2006, *Geophys. Res. Lett.*, *35*, L24605, doi:10.1029/2008GL036372.
Gordon, A. L., J. Sprintall, H. M. van Aken, D. Susanto, S. E. Wijffels, R. Molcard, A. Ffield, W. Pranowo, and S. Wirasantosa (2010), The Indonesian Throughflow during 2004–2006 as observed by the INSTANT program, *Dyn. Atmos. Oceans*, *50*(2), 115–128, doi:10.1016/j.dynatmoce.2009.12.002.
Gordon, A. L., B. A. Huber, E. J. Metzger, R. D. Susanto, H. E. Hurlburt, and T. R. Adi (2012), South China Sea Throughflow impact on the Indonesian Throughflow, *Geophys. Res. Lett.*, *39*, L11602, doi:10.1029/2012GL052021.
Hautala, S. L., J. L. Reid, and N. Bray (1996), The distribution and mixing of Pacific water masses in the Indonesian Seas, *J. Geophys. Res.*, *101*(C5), 12,375–12,389, doi:10.1029/96JC00037.
Hirst, A. C., and J. S. Godfrey (1993), The role of Indonesian Throughflow in a Global Ocean Gcm, *J. Phys. Oceanogr.*, *23*(6), 1057–1086.
Holbrook, N. J., I. D. Goodwin, S. McGregor, E. Molina, and S. B. Power (2011), ENSO to multi-decadal time scale changes in East Australian Current transports and Fort Denison sea level: Oceanic Rossby waves as the connecting mechanism, *Deep Sea Res., Part II*, *58*(5), 547–558, doi:10.1016/j.dsr2.2010.06.007.
Koch-Larrouy, A., M. Lengaigne, P. Terray, G. Madec, and S. Masson (2009), Tidal mixing in the Indonesian Seas and its effect on the tropical climate system, *Clim. Dyn.*, *34*(6), 891–904, doi:10.1007/s00382-009-0642-4.
Large, W. G., and S. G. Yeager (2009), The global climatology of an interannually varying air–sea flux data set, *Clim. Dyn.*, *33*(2–3), 341–364, doi:10.1007/s00382-008-0441-3.
Le Bars, D., H. A. Dijkstra, and W. P. M. de Ruijter (2013), Impact of the Indonesian Throughflow on Agulhas leakage, *Ocean Sci.*, *9*(5), 773–785, doi:10.5194/os-9-773-2013.
Lee, T., I. Fukumori, D. Menemenlis, Z. Xing, and L.-L. Fu (2002), Effects of the Indonesian Throughflow on the Pacific and Indian Oceans, *J. Phys. Oceanogr.*, *32*(5), 1404–1429.
Madec, G. (2008), *NEMO Ocean Engine—Version 3.2*, Inst. Pierre-Simon Laplace, Paris, France.
McClean, J. L., D. P. Ivanova, and J. Sprintall (2005), Remote origins of interannual variability in the Indonesian Throughflow region from data and a global Parallel Ocean Program simulation, *J. Geophys. Res.*, *110*, C10013, doi:10.1029/2004JC002477.
McCreary, J. P., Jr., T. Miyama, R. Furue, T. Jensen, H.-W. Kang, B. Bang, and T. Qu (2007), Interactions between the Indonesian Throughflow and circulations in the Indian and Pacific Oceans, *Prog. Oceanogr.*, *75*(1), 70–114, doi:10.1016/j.pocean.2007.05.004.
Meyers, G. (1996), Variation of Indonesian Throughflow and the El Niño Southern Oscillation, *J. Geophys. Res.*, *101*, 12,255–12,263.
Molcard, R., M. Fieux, and A. G. Ilahude (1996), The Indo-Pacific Throughflow in the Timor Passage, *J. Geophys. Res.*, *101*, 12,411–12,420.
Paris, C. B., J. Helgers, E. van Sebille, and A. Srinivasan (2013), Connectivity modeling system: A probabilistic modeling tool for the multi-scale tracking of biotic and abiotic variability in the ocean, *Environ. Modell. Software*, *42*(C), 47–54, doi:10.1016/j.envsoft.2012.12.006.
Potemra, J. T., and N. Schneider (2007), Interannual variations of the Indonesian Throughflow, *J. Geophys. Res.*, *112*, C05035, doi:10.1029/2006JC003808.
Ridgway, K. R., and J. R. Dunn (2003), Mesoscale structure of the mean East Australian Current System and its relationship with topography, *Prog. Oceanogr.*, *56*(2), 189–222, doi:10.1016/S0079–6611(03)00004-1.
Ridgway, K. R., and J. R. Dunn (2007), Observational evidence for a Southern Hemisphere oceanic supergyre, *Geophys. Res. Lett.*, *34*, L13612, doi:10.1029/2007GL030392.
Rintoul, S. R., and S. Sokolov (2001), Baroclinic transport variability of the Antarctic Circumpolar Current south of Australia (WOCE repeat section SR3), *J. Geophys. Res.*, *106*, 2815–2832.
Rosell-Fieschi, M., S. R. Rintoul, J. Gourrion, and J. L. Pelegrí (2013), Tasman Leakage of intermediate waters as inferred from Argo floats, *Geophys. Res. Lett.*, *40*, 5456–5460, doi:10.1002/2013GL057797.
Santoso, A., W. Cai, M. H. England, and S. J. Phipps (2011), The role of the Indonesian Throughflow on ENSO dynamics in a coupled climate model, *J Clim.*, *24*(3), 585–601, doi:10.1175/2010JCLI3745.1.
Santoso, A., M. H. England, and W. Cai (2012), Impact of Indo-Pacific feedback interactions on ENSO dynamics diagnosed using ensemble climate simulations, *J. Clim.*, *25*(21), 7743–7763, doi:10.1175/JCLI-D-11–00287.1.
Schwarzkopf, F. U., and C. W. Böning (2011), Contribution of Pacific wind stress to multi-decadal variations in upper-ocean heat content and sea level in the tropical south Indian Ocean, *Geophys. Res. Lett.*, *38*, L12602, doi:10.1029/2011GL047651.
Song, Q., G. A. Vecchi, and A. J. Rosati (2007), The role of the Indonesian Throughflow in the Indo–Pacific climate variability in the GFDL coupled climate model, *J. Clim.*, *20*(11), 2434–2451, doi:10.1175/JCLI4133.1.
Speich, S., B. Blanke, P. de Vries, S. S. Drijfhout, K. Döös, A. Ganachaud, and R. Marsh (2002), Tasman leakage: A new route in the global ocean conveyor belt, *Geophys. Res. Lett.*, *29*(10), 1416, doi:10.1029/2001GL014586.
Speich, S., B. Blanke, and W. Cai (2007), Atlantic meridional overturning circulation and the Southern Hemisphere supergyre, *Geophys. Res. Lett.*, *34*, L23614, doi:10.1029/2007GL031583.
Sprintall, J., S. Wijffels, A. L. Gordon, A. Ffield, R. Molcard, R. D. Susanto, I. Soesilo, J. Sopaheluwakan, Y. Surachman, and H. M. van Aken (2004), INSTANT: A new international array to measure the Indonesian Throughflow, *Eos Trans. AGU*, *85*(39), 369–376, doi:10.1029/2004EO390002.
Sprintall, J., S. E. Wijffels, R. Molcard, and I. Jaya (2009), Direct estimates of the Indonesian Throughflow entering the Indian Ocean: 2004–2006, *J. Geophys. Res.*, *114*, C07001, doi:10.1029/2008JC005257.
Susanto, R. D., A. Ffield, A. L. Gordon, and T. R. Adi (2012), Variability of Indonesian Throughflow within Makassar Strait, 2004–2009, *J. Geophys. Res.*, *117*, C09013, doi:10.1029/2012JC008096.
Susanto, R. D., Z. Wei, R. T. Adi, B. Fan, S. Li, and G. Fang (2013), Observations of the Karimata Strait Throughflow from December 2007 to November 2008, *Acta Oceanol. Sin.*, *32*(5), 1–6, doi:10.1007/s13131-013-0307-3.
Suthers, I. M., et al. (2011), The strengthening East Australian Current, its eddies and biological effects—An introduction and overview, *Deep Sea Res., Part II*, *58*(5), 538–546, doi:10.1016/j.dsr2.2010.09.029.
Talley, L. D. (2008), Freshwater transport estimates and the global overturning circulation: Shallow, deep and throughflow components, *Prog. Oceanogr.*, *78*(4), 257–303, doi:10.1016/j.pocean.2008.05.001.
Talley, L. D., and J. Sprintall (2005), Deep expression of the Indonesian Throughflow: Indonesian intermediate water in the South Equatorial Current, *J. Geophys. Res.*, *110*, C10009, doi:10.1029/2004JC002826.

Valsala, V., S. Maksyutov, and R. Murtugudde (2011), Interannual to interdecadal variabilities of the Indonesian Throughflow source water pathways in the Pacific Ocean, *J. Phys. Oceanogr.*, *41*(10), 1921–1940, doi:10.1175/2011JPO4561.1.

Valsala, V. K., and M. Ikeda (2007), Pathways and effects of the Indonesian Throughflow water in the Indian Ocean using particle trajectory and tracers in an OGCM, *J. Clim.*, *20*(13), 2994–3017, doi:10.1175/JCLI4167.1.

van Sebille, E., C. N. Barron, A. Biastoch, P. J. van Leeuwen, F. C. Vossepoel, and W. P. M. de Ruijter (2009), Relating Agulhas leakage to the Agulhas Current retroflection location, *Ocean Sci.*, *5*(4), 511–521.

van Sebille, E., P. J. van Leeuwen, A. Biastoch, and W. P. M. de Ruijter (2010), Flux comparison of Eulerian and Lagrangian estimates of Agulhas leakage: A case study using a numerical model, *Deep Sea Res., Part I*, *57*(3), 319–327, doi:10.1016/j.dsr.2009.12.006.

van Sebille, E., M. H. England, J. D. Zika, and B. M. Sloyan (2012), Tasman leakage in a fine-resolution ocean model, *Geophys. Res. Lett.*, *39*, L06601, doi:10.1029/2012GL051004.

van Sebille, E., P. Spence, M. R. Mazloff, M. H. England, S. R. Rintoul, and O. A. Saenko (2013), Abyssal connections of Antarctic Bottom Water in a Southern Ocean State estimate, *Geophys. Res. Lett.*, *40*, 2177–2182, doi:10.1002/grl.50483.

Vranes, K., A. L. Gordon, and A. Ffield (2002), The heat transport of the Indonesian Throughflow and implications for the Indian Ocean heat budget, *Deep Sea Res., Part II*, *49*(7–8), 1391–1410.

Wajsowicz, R. C., and E. K. Schneider (2001), The Indonesian Throughflow's effect on global climate determined from the COLA coupled climate system, *J. Clim.*, *14*(13), 3029–3042.

Wijffels, S., and G. Meyers (2004), An intersection of oceanic waveguides: Variability in the Indonesian Throughflow region, *J. Phys. Oceanogr.*, *34*(5), 1232–1253.

Yuan, D., J. Wang, T. Xu, P. Xu, Z. Hui, X. Zhao, Y. Luan, W. Zheng, and Y. Yu (2011), Forcing of the Indian Ocean Dipole on the Interannual variations of the Tropical Pacific Ocean: Roles of the Indonesian Throughflow, *J. Clim.*, *24*(14), 3593–3608, doi:10.1175/2011JCLI3649.1.